Biotechnology and Bioprocess Engineering 16: 13-22 (2011)
DOI 10.1007/s12257-010-0176-y

RESEARCH PAPER

A Simple Metabolic Flux Balance Analysis of Biomass and Bioethanol Production in *Saccharomyces cerevisiae* Fed-batch Cultures

Iliana Barrera-Martínez, R. Axayácatl González-García, Edgar Salgado-Manjarrez, and Juan S. Aranda-Barradas

Received: 2 June 2010 / Revised: 23 July 2010 / Accepted: 1 August 2010

Abstract Production of *Saccharomyces cerevisiae* yeast for applications in the food industry or in bioethanol production still presents important techno-economic challenges as an industrial bioprocess. Mathematical modeling of cellular metabolism in biological production usually improves process yields, though for industrial applications, the model should be as simple as possible in order to sustain model usefulness and technical feasibility. A comparative analysis between a black box description and a simple metabolic network accounting for the main metabolic events involved in yeast growth and bioethanol production is proposed here. In both cases, a thorough analysis of reaction rates allowed for the ethanol concentrations produced in fed-batch yeast cultures, although our results showed more accurate estimations with the metabolic flux balance methodology. Moreover, an interpretation of the yeast physiological state in fed-batch cultures at different glucose feed concentrations was accomplished by means of a stoichiometric analysis linked to the simplified metabolic network. The results confirmed that increasing glucose uptake rates, controlled mainly by the glucose concentration in the input flow, produced an up-regulation in reductive catabolism, resulting in higher ethanol excretion. The biomass production relied mostly on oxidative catabolism, which is controlled by the glucose and oxygen uptake rates. Thus, ethanol or biomass production is strongly dependent on the physiological state of yeast in the culture, which can be inferred from a suitable metabolic flux balance approach.

Iliana Barrera-Martínez, R. Axayácatl González-García, Edgar Salgado-Manjarrez, Juan S. Aranda-Barradas*
Department of Bioengineering, Professional Unit of Biotechnology, National Polytechnic Institute of Mexico, CP 07340, Mexico
Tel: +01-55-5729-6000+56347, Fax: +01-55-5729-6000+56305
E-mail: jaranda@ipn.mx

Keywords: bioethanol, biomass, metabolic flux balance, stoichiometric model, *Saccharomyces cerevisiae*

1. Introduction

The yeast *Saccharomyces cerevisiae* has been extensively used for the industrial bioconversion of carbohydrates from sugar cane and other agricultural materials (plant biomass). *S. cerevisiae* is used as feedstock for several food industry processes [1], and for the production of bio-alcohols, that are used as solvents, fuels or basic chemicals [2]. It must be stressed that controlled fed-batch strategies have been continuously proposed in order to reach optimal yields for yeast biomass production [3], while processes for ethanol production as a biofuel are still under research to fulfill requirements for economic competitiveness [4,5] without affecting global food supplies [6]. A rational way to achieve these goals is through the mathematical modeling of production processes.

The industrial production of yeast biomass and bioethanol have been technically improved in the past by application of modeling strategies [3,7], because mathematical models are useful to understand, predict, control or even design biological production systems [8]. Undoubtedly, effective mathematical modeling of biomass or ethanol production must involve biochemical pathways of central carbon metabolism, *i.e*, glycolysis, the tricarboxylic acid cycle and oxidative phosphorylation. Important contributions from the Constrained-based Modeling Paradigm (CMP) regarding large-scale metabolic networks based on annotated genomes have been reported [9-13], but industrial applications require metabolic models to be as simple as possible, and thus characterized by a reduced number of biochemical reactions. Some efforts on this condensed reac-

tions approach have provided interesting results about cell physiological conditions, kinetic behavior or process global performance with different microbial systems [14,15]. A simple metabolic flux balance (MFB) model has been suggested to study transient regulations of central carbon metabolism in *S. cerevisiae* [16], but no special emphasis was given to bioethanol or yeast biomass production in the culture. The integration of metabolic fluxes for explicit biomass production linked to oxidative phosphorylation, and for ethanol production from reductive metabolism, is proposed here in a simplified metabolic network to estimate ethanol and yeast biomass in fed-batch production processes.

2. Materials and Methods

2.1. Microorganism, media composition, and culture conditions

A commercial *S. cerevisiae* strain was grown in culture media with the following composition (g/L): KH_2PO_4 (7.0), $CaCl_2{\cdot}2H_2O$ (0.25), NaCl (0.5), and $MgCl_2{\cdot}6H_2O$ (6.0). Solutions of minerals and vitamins were added (10 mL/L each) and prepared as follows. Five hundred milliliters of mineral solution were prepared with: $FeSO_4{\cdot}7H_2O$ (278 mg), $ZnSO_4{\cdot}7H_2O$ (288 mg), $CuSO_4{\cdot}5H_2O$ (7.5 mg), $Na_2MoO_4{\cdot}2H_2O$ (25 mg), $MnSO_4{\cdot}H_2O$ (169 mg), and H_2SO_4 as needed to dissolve the Fe salt. Five hundred milliliters of vitamin solution contained: Biotin (1.5 mg), calcium pantothenate (20 mg), inositol (125 mg), pyridoxine-HCl (25 mg), and thiamine-HCl (50 mg). Glucose was supplied at three different concentrations (g/L) 27.2, 38.5, 50.0 for different experiments. The pH of the culture was controlled with ammonia-water solution (20% v/v), which was the only nitrogen source. Experimental culture conditions were: 30°C, pH 5.0, air flow 450 L/h, and dissolved oxygen at 10% of saturation value (*ca.* 0.8 mg/L).

2.2. Fed-batch yeast cultures

A 15 L bioreactor was used for all fed-batch experiments. Yeast cultures were inoculated using 3.0×10^6 cells/mL in a 6 L batch, and feeding started at 12 h post-inoculation with different glucose concentrations. Medium input flow was controlled at ~0.4 L/h to maintain glucose concentrations at approximately zero inside the bioreactor ($S \approx 0$), and favor substrate conversion.

A general mass balance on compound (z) for a fed-batch bioreactor is:

$$\frac{dz}{dt} = D(z_F - z) \pm q_Z \tag{1}$$

which can be arranged to estimate volumetric rates from concentration measurements as:

$$q_Z = \frac{dz}{dt} \pm D(z_F - z) \tag{2}$$

The first right-hand term in Eq. (2) vanishes as a steady state is approached, but the importance of this term is substance (z) and time (t) dependent. Therefore, for the experimental condition of the substrate that $S \approx 0$, a quasi-steady state is established ($dS/dt \approx 0$), and the glucose consumption rate is given by:

$$q_S = -D\,S_F \tag{3}$$

Whereas for the volumetric growth rate, dynamics are slower and it is more adequately calculated from:

$$q_X = \frac{dX}{dt} + DX \tag{4}$$

Or for a finite time interval:

$$q_X = \frac{\Delta X}{\Delta t} + D\overline{X} \tag{5}$$

In fact, Eq. (5) is also useful to estimate the volumetric rates for ethanol production and ammonia consumption, though the dilution term for the latter must not be taken into account because ammonia is instantaneously consumed after addition. An estimation of the biomass concentration in the liquid medium at any time in the culture can be roughly achieved if the specific growth rate (μ) is kept approximately constant:

$$X_{i+1} = X_i + \mu\,\overline{X}\,\Delta t \tag{6}$$

The oxygen consumption rate can be estimated when dissolved oxygen is exhausted in the liquid medium ($c_{O_2} \approx 0$) through the following expression:

$$q_{O_2} = -k_L a \cdot c^*_{O_2}$$

The mass transfer coefficient was both experimentally measured by means of a dynamic gassing-out method [17,18], and theoretically estimated with an empirical correlation [19].

2.3. Analytical techniques

Samples were taken every two hours for quantitative determinations. Biomass concentration in the sample was evaluated using an empirical correlation between dry weight and optical density measured at 620 nm (Boeco S-22, Hamburg, Germany). The sample was centrifuged for 5 min at 5,000 rpm (Sol-BAT, Puebla, Mexico), and glucose, ammonia, and ethanol concentrations were measured in the supernatant. The glucose and ammonia concentrations were quantified through spectrophotometric techniques (DNS reagent method and Nessler reagent method, respectively),

while bioethanol concentrations were measured by HPLC (TSP Spectra system, San Jose California, USA) with an Aminex HPX-87 column (Bio-Rad, Hercules California, USA) at 40°C, 1,200 psi, and a 0.4 mL/min mobile phase (H_2SO_4 5.0 mM) flow. From these experimental measurements, volumetric rates for ethanol production and ammonia consumption needed for a redundancy analysis were easily assessed. The outlet gas composition was continuously monitored using a paramagnetic oxygen analyzer (Servomex 570/571, Huston Texas, USA) and an infrared carbon dioxide analyzer (Servomex 1410, Huston Texas, USA) connected to a microcomputer, and the experimental respiratory quotient *RQ* was continuously monitored using this data.

2.4. Mathematical aspects

An aerobic culture of *S. cerevisiae* yeast with glucose (CH_2O), ammonia (NH_3) and dissolved oxygen (O_2) as substrates is represented by a black box description in the following form:

$$CH_2O + NH_3 + O_2 \rightarrow CH_{1.8}O_{0.58}N_{0.16} + CH_3O_{0.5} + CO_2 + H_2O \quad (8)$$

Main reaction products are yeast biomass ($CH_{1.8}O_{0.58}N_{0.16}$) and ethanol ($CH_3O_{0.5}$). The vector ($\boldsymbol{q}$) of volumetric reaction rates associated to Eq. (8) is:

$$\boldsymbol{q} = [q_S\ q_{NH_3}\ q_{O_2}\ q_X\ q_E\ q_{CO_2}\ q_{H_2O}]^T \quad (9)$$

Following a degree of freedom analysis [20], three reaction rates from vector $\boldsymbol{q}$ can be measured in order to estimate the remaining four. By defining a subvector of measured rates as $\boldsymbol{q}_m = [q_S\ q_X\ q_{O_2}]^T$, and a subvector of calculated rates as $\boldsymbol{q}_c = [q_{NH_3}\ q_E\ q_{CO_2}\ q_{H_2O}]^T$, vector $\boldsymbol{q}$ is restated as $\boldsymbol{q} = [\boldsymbol{q}_m\ \boldsymbol{q}_c]^T$. The black box model is then written as [20]:

$$\boldsymbol{q}_c = -[\boldsymbol{E}_c^{-1}\ \boldsymbol{E}_m]\ \boldsymbol{q}_m \quad (10)$$

where,

$$\boldsymbol{E} = [\boldsymbol{E}_m\ \boldsymbol{E}_c];\ \text{with}\ \boldsymbol{E}_m = \begin{bmatrix} 1 & 1 & 0 \\ 2 & 1.82 & 0 \\ 1 & 0.58 & 2 \\ 0 & 0.16 & 0 \end{bmatrix};\ \text{and}\ \boldsymbol{E}_c = \begin{bmatrix} 0 & 1 & 1 & 0 \\ 3 & 3 & 0 & 2 \\ 0 & 0.5 & 2 & 1 \\ 1 & 0 & 0 & 0 \end{bmatrix} \quad (11)$$

$\boldsymbol{E}$ is the elemental matrix associated to Eq. (8) [20,21]. The kinetic system is overdetermined whenever more than D_F rates are measured, and then a redundancy analysis can be performed. Such an analysis allows for the estimation of gross errors in experimental measurements, as explained in the appendix.

A more detailed description of the biochemical processes involved in yeast aerobic growth and ethanol excretion is obtained from metabolic flux balance (MFB). In this approach [25], a reduced stoichiometric description of the involved biochemical pathways for global biomass or ethanol production is considered for evaluating the performance of the process. Such a condensed metabolic network is presented in Fig. 1. The volumetric rates ($\boldsymbol{q}$) now depend on the specific reaction rate (r_j) for each biochemical reaction in the metabolic network according to [26]:

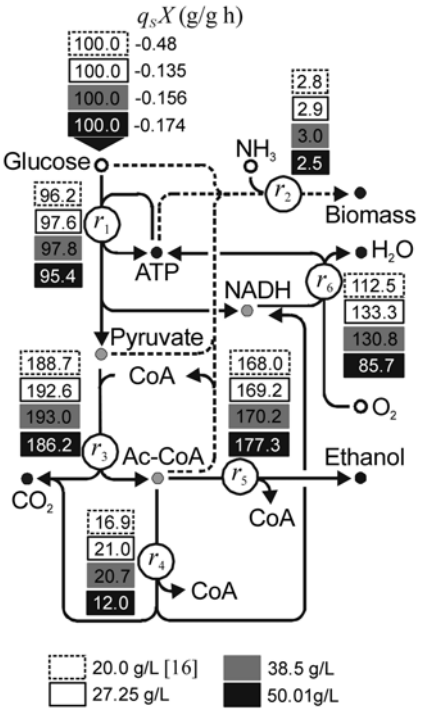

Fig. 1. A minimal metabolic network for a yeast culture producing biomass and bioethanol. Metabolic fluxes for different glucose concentrations in the fed stream (27.2, 38.5, and 50.0 g/L) are referred to the glucose uptake rate (100%) and compared with data from [16] (20.0 g/L).

$$\boldsymbol{q} = \boldsymbol{T}^T\ \boldsymbol{r}\ X \quad (12)$$

where $\boldsymbol{T}^T$ is the transpose of the total stoichiometric matrix. Eq. (12) is conveniently partitioned in a manner similar to Eq. (11) as follows:

$$\begin{pmatrix} \boldsymbol{q}_m \\ \boldsymbol{q}_c \\ 0 \end{pmatrix} = \begin{pmatrix} \boldsymbol{T}_1\boldsymbol{T}_2 \\ \boldsymbol{T}_3\boldsymbol{T}_4 \\ \boldsymbol{T}_5\boldsymbol{T}_6 \end{pmatrix} \begin{pmatrix} \boldsymbol{r}_m X \\ \boldsymbol{r}_c X \end{pmatrix} \quad (13)$$

Vectors $\boldsymbol{r}_m = [r_5\ r_4\ r_3]^T$ and $\boldsymbol{r}_c = [\ r_2\ r_1\ r_6]^T$ are the unknown metabolic fluxes in the network. Considering the so-called quasi-steady state assumption in the CMP [25], one can derive from Eq. (13) the unknown fluxes $\boldsymbol{r}_m$ and $\boldsymbol{r}_c$, as shown in the appendix:

$$\boldsymbol{r}_m X = \boldsymbol{A}_m \boldsymbol{q}_m,\ \text{where}\ \boldsymbol{A}_m = [\boldsymbol{T}_1 - \boldsymbol{T}_2\boldsymbol{T}_6^{-1}\boldsymbol{T}_5]^{-1} \quad (14)$$

and,

$\boldsymbol{r}_c X = \boldsymbol{A}_c \boldsymbol{q}_m$, where $\boldsymbol{A}_c = -\boldsymbol{T}_6^{-1}\boldsymbol{T}_5[\boldsymbol{T}_1 - \boldsymbol{T}_2\boldsymbol{T}_6^{-1}\boldsymbol{T}_5]^{-1}$ (14)

For the MFB in a yeast biomass or ethanol production process (Fig. 1), matrices $\boldsymbol{A}_m$ and $\boldsymbol{A}_c$ are:

$$\boldsymbol{A}_m = \begin{bmatrix} 0 & 0.091 & 0 \\ -1 & -0.091 & 0 \\ 0 & 0.000 & -2 \end{bmatrix}; \text{ and } \boldsymbol{A}_c = \begin{bmatrix} -2 & -0.318 & 0.333 \\ 0 & -0.045 & -0.333 \\ -2 & -0.273 & 0.000 \end{bmatrix} \quad (16)$$

3. Results and Discussion

3.1. Biomass and bioethanol production in fed-batch cultures

Fig. 2 shows the yeast kinetic behavior in glucose fed-batch processes at various feed concentrations. A general trend indicated that high glucose uptake rates resulted in low amounts of biomass generation, and higher ethanol production. This is also verified in the biomass ($Y_{X/S}$) and ethanol ($Y_{E/S}$) yield coefficients presented in Table 1. Since ethanol excretion was higher with larger substrate availability, even in aerobic conditions, this data indicates that reductive catabolism in yeast cells was further activated to some extent. Interestingly, these observations correspond to the measured and estimated RQ values for the different fed-batch processes (Fig. 3). In a batch process where $S >> 0$, there is an important CO_2 production from pyruvate decarboxylation, with a simultaneous ethanol production at the maximal O_2 consumption, and the respiratory quotient is > 1. If glucose concentration in the culture medium is controlled through a fed-batch process ($S \approx 0$), CO_2 production is stoichiometrically equivalent to O_2 consumption and $RQ \approx 1$ [27]. However, if glucose in the feed exceeds the yeast respiratory capacity [28], a slightly increasing trend in the respiratory quotient is observed, as noted in Fig. 3. As a consequence, ethanol concentrations in the bioreactor are also higher (Fig. 2). Although biomass and bioethanol accumulation occur simultaneously in a yeast culture, metabolism can be controlled to induce either product.

3.2. Analysis of reaction rates for bioethanol production using a black box description

From the biomass experimental concentrations and the feed glucose concentrations, instantaneous volumetric rates, q_S and q_X, were calculated through Eqs. (3) and (5), respectively. In addition, the mass transfer coefficient was either measured or estimated as a function of the aeration flow (Q_G), and the correlation is shown in Fig. 4. At the air flow established in the experiments, we found that $k_La = 51.9$/h according to the empirical correlation by Moresi and Patete [19], therefore, from Eq. (7), the essentially constant oxygen consumption rate was $q_{O_2} = 0.416$ g/L/h. According to the black box description, the measured volumetric rates allowed for the estimation of ethanol production rate (q_E) during culture, so instantaneous ethanol concentrations can be predicted from:

$$E_{i+1} = E_i + q_E \Delta t \quad (17)$$

where an initial experimental value (E_0) is needed to start the estimation of the subsequent ethanol concentrations. Upper and lower confidence bounds for the predicted concentrations were obtained with error (δ_E) resulting from the redundancy analysis (see appendix section):

$$\begin{aligned} E_{i+1,upper} &= E_i + (q_E + \delta_E)\Delta t \\ E_{i+1,lower} &= E_i - (q_E - \delta_E)\Delta t \end{aligned} \quad (18)$$

As it can be observed in ethanol plots (Fig. 2), ethanol concentration in fed-batch processes was acceptably depicted by a black box approach. Nonetheless, ethanol estimations are substantially improved by considering the main metabolic events in conversion of glucose to both yeast biomass and bioethanol.

3.3. Metabolic flux distributions for a simplified metabolic network in *S. cerevisiae*

A simplified metabolic network to describe cellular growth and ethanol production in fed-batch processes is proposed in Fig. 1. Metabolic flux (r_1) represents the glucose flow through glycolysis until pyruvate, which is decarboxylated to acetyl-CoA in flux (r_3). This two-carbon intermediary is either converted to ethanol through metabolic flux (r_5), or incorporated to a simplified Krebs cycle in flux (r_4). The fluxes r_4 and r_5 correspond, respectively, to the activities of oxidative and reductive catabolism in the yeast cells. The metabolic flux (r_6) represents the activity level in the respiratory chain and the rate of NADH oxidation, while r_2 indicates a condensed biomass synthesis from the key intermediaries: glucose, pyruvate, and acetyl-CoA. Table 2 shows the stoichiometry associated with this minimal metabolic network. Given that glucose supply in the fed-batch cultures was controlled to match the experimental condition ($S \approx 0$), the specific growth rate (μ) shifted gradually toward the dilution rate, D 0.1/h, so the fed-batch culture approached a continuous culture behavior. For this reason, volumetric rates for production or consumption in the fed-batch processes were practically constant, therefore giving consistent distributions of calculated metabolic fluxes Fig. 1. This simplified modeling approach was further validated by using data from Herwig and von Stockar [16]. Although their metabolic flux model was proposed to properly describe transient metabolic behavior in *S. cerevisiae*, they presented some experimental data under steady state conditions, at $D = 0.245$/h, which can be used to

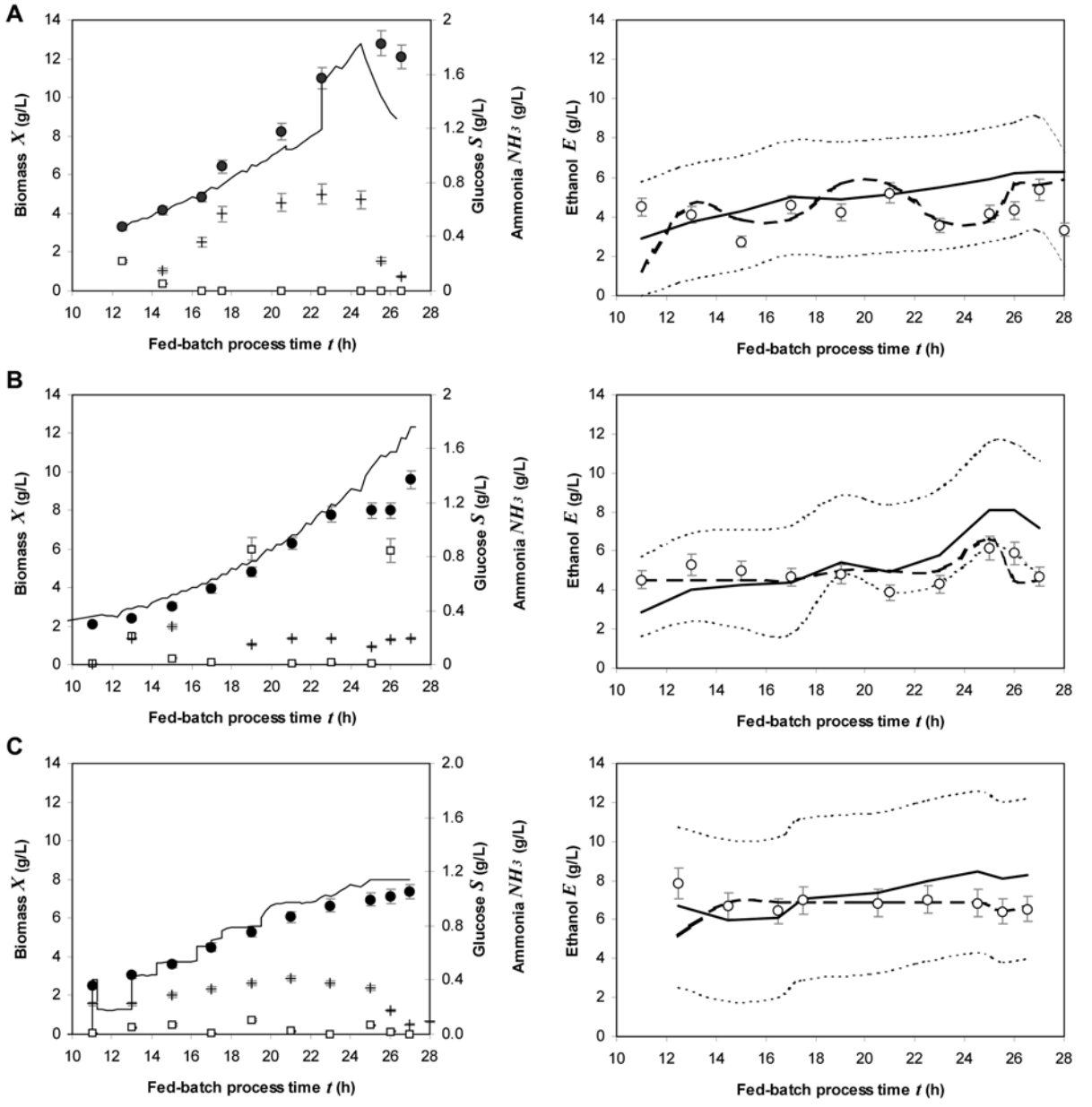

Fig. 2. Produced biomass (●), residual glucose (□), consumed ammonia (+), and produced ethanol (○) concentrations experimentally measured for yeast fed-batch cultures with different glucose supplies in the feed (g/L): (A) 27.2, (B) 38.5, and (C) 50.0. Estimated biomass concentrations (Eq. (6)) are also included (———). Ethanol plots present the concentrations predicted by a black box description (▬▬) with the corresponding estimated error (·····), and by a metabolic flux balance analysis (▬ ▬).

calculate $\boldsymbol{q}_m$ = [–4.8 2.01 –2.7]. These volumetric rates were then introduced in Eqs. (14) and (15) in order to evaluate the flux distributions, which are included in Fig. 1. The results are consistent with our flux distributions, except perhaps for r_6, which is underestimated to some extent. This underestimation of the NADH oxidation flux is attributed to the lower oxygen content considered in biomass composition in the model by Herwig and von Stockar [16].

The metabolic fluxes involved in ethanol production allowed for the estimation of ethanol concentrations included in ethanol plots in Fig. 2, where it can be seen that the predicted values improved estimations from the black box

Table 1. Yield coefficients for fed-batch cultures at different glucose concentrations in the feed

Glucose supply concentration (g/L)	Final biomass concentration (g/L)	Final ethanol concentration (g/L)	Biomass yield (g/g)	Ethanol yield (g/g)
27.25	12.2	4.7	0.44	0.059
38.5	9.8	5.1	0.42	0.093
50.01	7.2	6.3	0.37	0.11

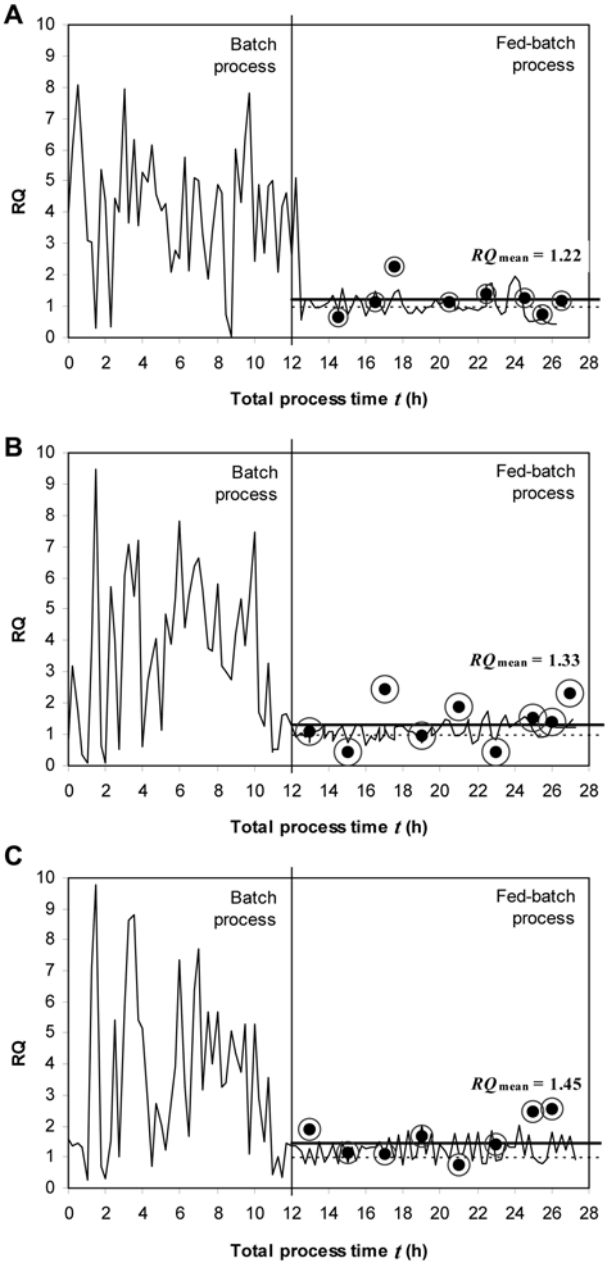

Fig. 3. Respiratory quotient *RQ* in yeast cultures for yeast fed-batch cultures with different glucose supplies in the feed (g/L): (A) 27.2, (B) 38.5, and (C) 50.0. Experimental data (———) and estimated (●) from black box reaction rates analysis. The mean estimated values are also shown (▬▬) for comparison with the fully oxidative theoretical value, *RQ* = 1 (·····). Circles surrounding the markers correspond to errors for *RQ* calculated from the redundancy analysis.

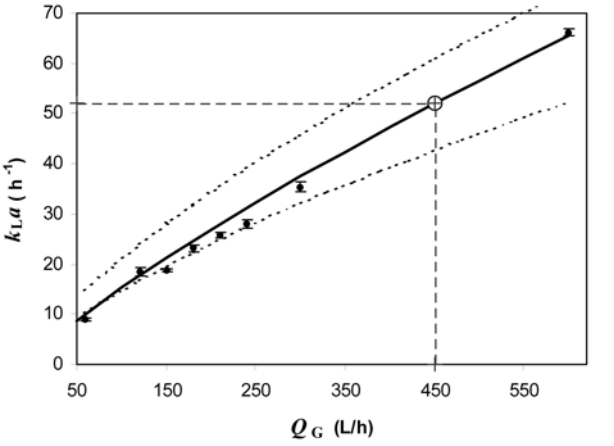

Fig. 4. Estimated (▬▬) and measured (●) oxygen transfer coefficients for the fed-batch culture system. The confidence interval for the estimated values is also shown (·····).

description and more closely reproduced the experimental measurements.

It should be noted from Fig. 1, that by increasing glucose concentration in the feed, the relative flux to biomass production (r_2) decreased, while the ethanol excretion, (r_5) was augmented. This would mean that yeast cells present a physiological adjustment to an excessive glucose uptake flow, resulting in a substantial activation of reductive catabolism (r_5), which is proportional to the glycolytic flux (r_1), as shown in Fig. 5B. The oxidative catabolism was also diminished for higher glucose concentrations in the feed, Fig. 5A. Thus, catabolic repression of NADH oxidation by glucose [29] was confirmed. Krebs cycle, flux (r_4), is considered here as a biochemical pathway, to some extent representative of oxidative catabolism. In Fig. 5C, one observes that the metabolic flux (r_4), associated with the tricarboxylic acid cycle, decreased for increasing glycolytic flux (r_1). Moreover, when reductive metabolism (r_5) increased (Fig. 5D), a diminishing trend in oxidative catabolism flux (r_4) was registered. These results are consistent with plots in Fig. 2 for the reduction in biomass concentrations and increase in ethanol concentrations as functions of available glucose in the feed.

Figs. 5A and 5C show that oxidative catabolism and NADH oxidation are higher with decreasing glucose concentration in the feed. Although this behavior is clearly observable in metabolic fluxes r_4 and r_6, it can be seen in Fig. 5B for reductive catabolism flux (r_5), that it is proportional to the glycolytic flux (r_1) in spite of the glucose concentration in the input flow. This finding implies different physiological responses of oxidative and reductive catabolism in yeast cells to a glucose uptake overflow. The reductive catabolism enhancement would result from the activation/inhibition of some existing enzymatic pool in the cytoplasm for pyruvate decarboxylation and reduction to ethanol, so this pool can quickly match any variation in the glucose uptake rate. In contrast, genetic expression/repression phenomena would be implied in oxidative catabolism because different fluxes are estimated in oxidative catabolism pathways for different glucose availability levels in the culture. The glucose uptake levels seem to be strong-

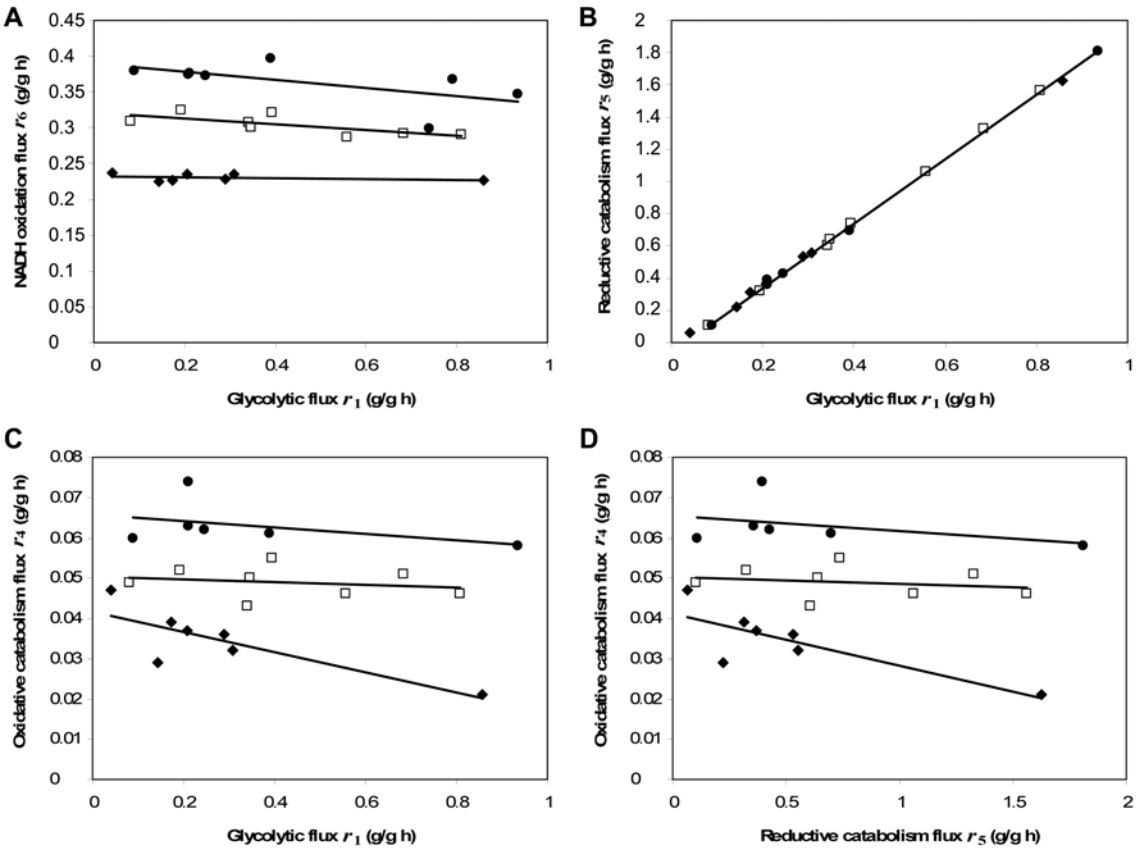

Fig. 5. Compared metabolic fluxes for oxidative and reductive catabolic pathways for yeast fed-batch cultures at (●) 27.2, (□) 38.5, and (◆) 50.0 g/L in the fed stream.

Table 2. Simplified stoichiometry for glucose conversion to biomass and ethanol by *S. cerevisiae*

Flux	Cellular process	Condensed reaction
r_1	Glycolysis	Glucose + $2H_3PO_4$ + 2ADP + $2NAD^+$ → 2Pyruvate + $2H_2O$ + 2ATP + 2NADH
r_2	Biomass production	Glucose + Pyruvate + Acetyl-CoA + NH_3 + 27.5ATP + $24.1H_2O$ → Biomass + CoA + 27.5ADP + $27.5H_3PO_4$
r_3	Pyruvate decarboxylation	Pyruvate + CoA + NAD + → Acetyl-CoA + CO_2 + NADH
r_4	Krebs cycle	Acetyl-CoA + $2H_2O$ + H_3PO_4 + ADP + $4NAD^+$ → $2CO_2$ + CoA + ATP + 4NADH
r_5	Ethanol production	Acetyl-CoA + H_3PO_4 + ADP + 2NADH → Ethanol + CoA + H_2O + ATP + $2NAD^+$
r_6	Respiratory chain	3ADP + $3H_3PO_4$ + NADH + $0.5O_2$ → 3ATP + NAD^+ + $4H_2O$

ly involved in the oxidative physiology of aerobic yeast cultures, and biomass and ethanol production yields depend on the glucose/oxygen uptake balance.

4. Conclusion

The experimental measurements needed for calculating the metabolic flux distributions included the accumulated biomass, consumed glucose, and consumed oxygen. From these data, glucose uptake, glycolytic flux, reductive catabolism, oxidative catabolism, and NADH oxidation rates were available through MFB in a biomass or bioethanol production process. The volumetric rate for biomass can be calculated from estimations of the biomass concentrations based on a constant specific growth rate (Eq. (6)), while glucose consumption rate depended on the dilution rate and the glucose concentration in the feed (Eq. (3)). Oxygen consumption rate depended on the oxygen saturation concentration and the mass transfer coefficient, k_La (Eq. (7)). The parameters needed for evaluating these volumetric rates are often known in aerobic fed-batch processes, so metabolic flux distributions can be easily estimated during process time, thereby presenting valuable information to develop optimized production processes for biomass or ethanol using *S. cerevisiae*.

Incorporating biochemical and metabolic events into the performance evaluation of a biomass or ethanol production process improved the estimation of process final concentrations and yields, regardless of the intended main product of the process. Moreover, the estimation of metabolic fluxes for oxidative and reductive catabolism in yeast cells is useful to achieve optimal yields from the process. For bioethanol production, the MFB analysis is also used for very accurate predictions of experimental concentrations. Therefore, the analysis of reaction rates in a minimal metabolic network provided important information about the physiology of cultured yeast cells, and the production of bioethanol or biomass could be improved by adjusting fed-batch experimental conditions. If bioethanol is the required product, a high subtrate supply rate should be established while maintaining the oxygen supply at low levels, although anaerobiosis must be avoided. In yeast biomass production processes, a more controlled glucose feed strategy with fully aerobic conditions will result in reduced overflow at the pyruvate level, and maximize the oxidative catabolism associated with high biomass yields.

Acknowledgements

This work was financially supported by the National Council for Science and Technology (CONACyT-Mexico) and the Research Office of the National Polytechnique Institute (SIP-IPN, Mexico). Authors kindly acknowledge these institutions for the provided funds and scholarships.

Nomenclature

C : Compounds in quasi-steady state [–]
$c^*_{O_2}$: Oxygen saturation concentration [mg/L]
c_{O_2} : Dissolved oxygen concentration in the bioreactor [mg/L]
D : Dilution rate in the fed-batch system [1/h]
D_F : Degrees of freedom [–]
$\boldsymbol{E}$: Elemental matrix [–]
$\boldsymbol{E}_c$, $\boldsymbol{E}_m$: Partitions of $\boldsymbol{E}$ [–]
E : Ethanol concentration in the bioreactor [g/L]
E_T : Total produced ethanol [g]
$\boldsymbol{F}$: Variance-covariance matrix [–]
J : Reactions considered in a metabolic network [–]
k_La : Oxygen transfer coefficient in the system [/h]
NH_3 : Consumed ammonia in the culture [g/L]
ne : Number of main elements in the global reaction (Eq. 5) [–]
np : Number of products in the global reaction (Eq. 5) [–]
ns : Number of substrates in the global reaction (Eq. 5) [–]
$\boldsymbol{P}$: Modified matrix of variance-covariance [–]
Q_G : Aeration flow to the bioreactor [L/h]
$\boldsymbol{q}$: Vector of volumetric rates [g/L h]
$\boldsymbol{q}_c$: Vector of calculated volumetric rates [g/L h]
$\boldsymbol{q}_m$: Vector of measured volumetric rates [g/L h]
$\boldsymbol{q}_{mt}$: Vector of true volumetric rates [g/L h]
q_E : Volumetric rate for ethanol production [g/L h]
q_{CO_2} : Volumetric rate for CO_2 production [g/L h]
q_{H_2O} : Volumetric rate for water production [g/L h]
q_{NH_3} : Volumetric rate for NH_3 consumption [g/L h]
q_{O_2} : Volumetric rate for oxygen consumption [g/L h]
q_S : Volumetric rate for glucose consumption [g/L h]
q_X : Volumetric rate of yeast growth [g/L h]
$\boldsymbol{R}$: Redundancy matrix [–]
$\boldsymbol{R}_r$: Reduced redundancy matrix [–]
RQ : Respiratory quotient [–]
$\boldsymbol{r}$: Vector of metabolic fluxes [g/g h]
$\boldsymbol{r}_c$, $\boldsymbol{r}_m$: Partitions of $\boldsymbol{r}$ [g/g h]
$\boldsymbol{T}$: Total stoichiometric matrix [–]
$\boldsymbol{T}_j$: Partitions of $\boldsymbol{T}^T$ (j = 1, ..., 6) [–]
S : Glucose concentration in the bioreactor [g/L]
S_F : Glucose concentration in the inlet stream [g/L]
S_T : Total consumed glucose [g]
t : Process time [h]
X : Biomass concentration in the bioreactor [g/L]
$Y_{E/S}$: Ethanol yield coefficient [g/g]
$Y_{X/S}$: Biomass yield coefficient [g/g]
$\bar{z}$: Mean value of z in the interval $z_{i+1} - z_i$ [l units]

Greek

$\Delta z = z_{i+1} - z_i$: Increment in variable z [l units]
δ : Vector of errors in measured rates [g/L h]
μ : Specific growth rate [1/h]

Superscripts

T : Transpose matrix [–]
-1 : Inverse matrix [–]

Subscripts

0 : Initial value or condition [–]
i : Initial point of a time interval [–]
i + 1 : Final point of a time interval [–]
j : Counter for the J reactions in the metabolic network [–]

Appendix

The global kinetics for an aerobic culture of *S. cerevisiae* is represented by a black box description in Eq. (8), and the volumetric reaction rates involved in the process are expressed in vector $\boldsymbol{q}$ (Eq. (9)). A kinetic description of the aerobic growth with ethanol production, as represented in

Eq. (8), is achieved by knowing the numerical values for the reaction rates in $\boldsymbol{q}$ during the microbial culture process. Reaction rate analysis consists of measuring some of the rates in vector $\boldsymbol{q}$ according to the degrees of freedom (D_F) associated with the kinetic description, and then in calculating the remaining unmeasured rates. The degrees of freedom are [20]:

$$D_F = ns + np + 1 - ne = 3 + 3 + 1 - 4 = 3 \quad \text{(A1)}$$

meaning that three reaction rates from vector $\boldsymbol{q}$ shall be measured in order to estimate the remaining four. Thus, $\boldsymbol{q}_m = [q_S\ q_X\ q_{O_2}]^T$ and $\boldsymbol{q}_c = [q_{NH_3}, q_E, q_{CO_2}, q_{H_2O}]^T$, where $\boldsymbol{q}_m$ is the subvector containing the measured rates and $\boldsymbol{q}_c$ is the subvector of calculated reaction rates.

Considering $\boldsymbol{E}$ as the elemental matrix related to Eq. (8), it can be shown, by the law of mass conservation [20,21], that:

$$\boldsymbol{E}\,\boldsymbol{q} = 0 \quad \text{(A2)}$$

The matrix $\boldsymbol{E}$ for the biomass production reaction Eq. (8) is expressed in a partitioned form $\boldsymbol{E}_m$ and $\boldsymbol{E}_c$, as shown in Eq. (11), in order to match the partition vector $\boldsymbol{q}$ previously stated. According to this, Eq. (A2) can be rewritten to give [20]:

$$\boldsymbol{E}\,\boldsymbol{q} = \boldsymbol{E}_m\boldsymbol{q}_m + \boldsymbol{E}_c\boldsymbol{q}_c = 0 \quad \text{(A3)}$$

and finally,

$$\boldsymbol{q}_c = -[\boldsymbol{E}_c^{-1}\boldsymbol{E}_m]\boldsymbol{q}_m \quad \text{(A4)}$$

which is the black box model for Eq. (8). If more than D_F rates are measured, the kinetic system is overdetermined, so a redundancy analysis can be performed to estimate gross experimental errors in measurements. The redundancy matrix is given by [22]:

$$\boldsymbol{R} = \boldsymbol{R}_m - \boldsymbol{E}_c[\boldsymbol{E}_c^T\boldsymbol{E}_c]^{-1}\boldsymbol{E}_c^T\boldsymbol{E}_m \quad \text{(A5)}$$

from which a reduced redundancy matrix $\boldsymbol{R}_r$ is defined by elimination of dependent rows in $\boldsymbol{R}$. Considering $\boldsymbol{q}_m$ as the measured rates corresponding to the true values $\boldsymbol{q}_{mt}$, it can be stated that $\boldsymbol{q}_m = \boldsymbol{q}_{mt} + \delta$, where δ is the vector of measurement errors, which can be calculated from [22,23]:

$$\delta = \boldsymbol{F}\,\boldsymbol{R}_r^T\,\boldsymbol{P}^{-1}\,\boldsymbol{R}_r\,\boldsymbol{q}_m \quad \text{(A6)}$$

Here, $\boldsymbol{F}$ is the variance-covariance matrix, and $\boldsymbol{P}$ is given by [24]:

$$\boldsymbol{P} = \boldsymbol{R}_r\boldsymbol{F}\,\boldsymbol{R}_r^T \quad \text{(A7)}$$

Thus, through the accurate estimations of q_E and q_{NH_3} from experimental data with Eq. (5) to get an overdetermined system, errors in $\boldsymbol{q}_m$ are actually calculated.

In a metabolic flux balance (MFB) description [25], a reduced stoichiometric network of the involved biochemical pathways for global biomass or ethanol production is considered for evaluating the performance of the process (Fig. 1). Biomass and ethanol production rates depend on the specific reaction rate (r_j) for each biochemical reaction in the simplified metabolic network as indicated in Eq. (12). From the matrix partition expressed in Eq. (13), it follows that:

$$\boldsymbol{q}_m = \boldsymbol{T}_1\boldsymbol{r}_m X + \boldsymbol{T}_2\boldsymbol{r}_c X, \quad \text{(A8)}$$

$$\boldsymbol{q}_c = \boldsymbol{T}_3\boldsymbol{r}_m X + \boldsymbol{T}_4\boldsymbol{r}_c X, \quad \text{(A9)}$$

and,

$$\boldsymbol{0} = \boldsymbol{T}_5\boldsymbol{r}_m + \boldsymbol{T}_6\boldsymbol{r}_c \quad \text{(A10)}$$

Eq. (A10) represents the so-called quasi-steady state assumption in the CMP [25]. By combining Eqs. (A8) ~ (A10), the unknown fluxes $\boldsymbol{r}_m = [r_5\ r_4\ r_3]^T$ and $\boldsymbol{r}_c = [\,r_2\ r_1\ r_6]^T$ can be calculated as indicated in Eqs. (14) ~ (16). In this MBF approach, the degrees of freedom are:

$$D_F = J - C = 6 - 3 = 3 \quad \text{(A11)}$$

where J is the number of reactions in the metabolic network, and C is the number of pathway intermediates in quasi-steady state. According to this, the measurement of volumetric rates $q_m = [q_S\ q_X\ q_{O_2}]^T$ provides sufficient experimental data to estimate a complete metabolic flux distribution $\boldsymbol{r} = [\boldsymbol{r}_m\ \boldsymbol{r}_c]^T$, in the minimal reaction set shown in Fig. 1, which represents the main physiological events during yeast growth and ethanol production.

References

1. Jørgensen, H., L. Olsson, B. Rønnow, and E. A. Palmqvist (2002) Fed-batch cultivations of baker's yeast followed by a nitrogen or carbon starvation: Effects on fermentative capacity and content of trehalose and glycogen. *App. Microbiol. Biotechnol.* 59: 310-317.
2. Antoni, D., V. Zverlov, and W. H. Schwarz (2007) Biofuels from microbes. *App. Microbiol. Biotechnol.* 77: 23-35.
3. Cannizzaro, C., S. Valentinotti, and U. von Stockar (2004) Control of yeast fed-batch process through regulation of extracellular ethanol concentration. *Bioproc. Biosys. Eng.* 26: 377-383.
4. Kwiatkowski, J. R., A. J. McAloon, F. Taylor, and D. B. Johnston (2006) Modeling the process and costs of fuel ethanol production by corn dry-grind process. *Indus. Crops Prod.* 23: 288-296.
5. Hahn-Hägerdal, B., M. Galbe, M. F. Gorwa-Grauslung, G. Lidén, and G. Zacchi (2006) Bio-ethanol – the fuel of tomorrow from the residues of today. *Trends Biotechnol.* 24: 549-556.
6. Hill, J., E. Nelson, D. Tilman, S. Polasky, and D. Tiffanty (2005) Environmental, economic, and energetic costs and benefits of biodiesel and ethanol biofuels. *Proc. Natl. Acad. Sci. USA* 103: 11206-11210.
7. Wong, W. Ch., H. -S. Song, J. H. Lee, and D. Ramkrishna (2010) Hybrid cybernetic model-based simulation of continuous produc-

tion of lignocellulosic ethanol: Rejecting abruptly changing feed conditions. *Contrl. Eng. Pract.* 18: 177-189.
8. Wu, W. H., F. Sh. Wang, and M. Sh. Chang (2008) Dynamic sensitivity analysis of biological systems. *BMC Bioinformatics* 9: 1-17.
9. Pricen, N. D., J. L. Reed, and B. O. Palsson (2004) Genome-scale models of microbial cells: Evaluating the consequences of constraints. *Nat. Rev. Microbiol.* 2: 886-897.
10. Mahadevan, R., A. P. Burgard, I. Famili, S.van Dien, and Ch. H. Schilling (2005) Applications of metabolic modelling to drive process development for the production of value-added chemicals. *Biotechnol. Bioproc. Eng.* 10: 408-417.
11. Hjersted, J. L., M. A. Henson, and R. Mahadevan (2007) Genome-scale analysis of *Saccharomyces cerevisiae* metabolism and ethanol production in fed-batch culture. *Biotechnol. Bioeng.* 97: 1190-1204.
12. Bro, Ch., B. Regenberg, J. Förster, and J. Nielsen (2006) *In silico* aided metabolic engineering of *Saccharomyces cerevisiae* for improved bioethanol production. *Metabolic Eng.* 8: 102-111.
13. Shiyota, S., H. Shimizu, T. Hirasawa, K. Nagahisa, C. Furusawa, G. Pandey, and Y. Katakura (2007) Metabolic pathway recruiting through genome data analysis for industrial application of *Saccharomyces cerevisiae*. *Biochem. Eng. J.* 36: 28-37.
14. Burgard, A. P., S. Vaidyaraman, and C. D. Maranas (2001) Minimal reaction sets for *Eschericha coli* metabolism under different growth requirements and uptake environments. *Biotechnolg. Prog.* 17: 791-797.
15. Aranda-Barradas, J. S., C. Garibay-Orijel, J. A. Badillo-Corona, and E. Salgado-Manjarrez (2010) A stochiometric analysis of biological xylitol production. *Biochem. Eng. J.* 50: 1-9.
16. Herwig, Ch. and U. von Stockar (2002) A small metabolic flux model to identify transient metabolic regulations in *Saccharomyces cerevisiae*. *Bioproc. Biosys. Eng.* 24: 395-403.
17. Merchuk, J. C., S. Yona, M. H. Siegel, and A. Ben Zvi (1989) On the first order approximation to the response of dissolved oxygen electrodes for dynamic k_La estimation. *Biotechnol. Bioeng.* 35: 1161-1163.
18. Scargiali, F., A. Busciglio, F. Grisafi, and A. Brucato (2010) Simplified dynamic pressure method for k_La measurements in aerated bioreactors. *Biochem. Eng. J.* 49: 165-172.
19. Moresi, M. and M. Patete (1988) Prediction of k_La in conventional stirred fermenters. *J. Chem. Tech. Biotechnol.* 42: 197-210.
20. Nielsen, J. and J. Villadsen (1994) *Bioreaction Engineering Principles*. pp. 100-102. Plenum Press, NY, USA.
21. Soto-Cruz, O. and J. Páez-Lerma (2005) Fermentation process balances: Consistency and metabolic flux analysis. *Rev. Mex. Ing. Quim.* 4: 59-74.
22. van der Heijden, R. T. J. M., B. Romein, J. J. Heijnen, C. Hellinga, and K. Luyben (1994) Linear constraint relations in biochemical reaction system: II. Diagnosis and estimation of gross errors. *Biotechnol. Bioeng.* 43: 11-20.
23. Nielsen, J. and J. Villadsen (1994) *Bioreaction Engineering Principles*. pp. 138-141. Plenum Press, NY, USA.
24. Stephanopoulos, G. N., A. A. Aristidou, and J. Nielsen (1998) *Metabolic Engineering Principles and Methodologies*. pp. 138-139. Academic Press, NY, USA.
25. Llaneras, F. and J. Picó (2008) Stoichiometric modelling of cell metabolism. *J. Biosci. Bioeng.* 105: 1-11.
26. Nielsen, J. and J. Villadsen (1994) *Bioreaction Engineering Principles*. pp. 111-116. Plenum Press, NY, USA.
27. Fiechter, A., G. F. Furhmann, and O. Käppeli (1981) Regulation of glucose metabolism in growing yeast cells. *Adv. Microbiol. Physiol.* 22: 123-183.
28. Cooney, Ch. L., H. Y. Wang, and D. I. C. Wang (1977) Computer-aided baker's yeast fermentations. *Biotech. Bioeng.* 19: 69-86.
29. Gancedo, J. M. (1998) Yeast carbon catabolite repression. *Microbiol. Mol. Biol. Rev.* 62: 334-361.